Low spin structure of the $N=Z$ odd-odd nucleus $^{54}_{27}Co_{27}$

I. Schneider,[1] A. F. Lisetskiy,[1] C. Frießner,[1] R. V. Jolos,[2] N. Pietralla,[1] A. Schmidt,[1] D. Weisshaar,[1] and P. von Brentano[1]
[1]*Institut für Kernphysik, Universität zu Köln, D-50937 Köln, Germany*
[2]*Bogoliubov Theoretical Laboratory, Joint Institute for Nuclear Research, 141980 Dubna, Russia*
(Received 23 June 1999; published 9 March 2000)

Low spin states in the odd-odd nucleus ^{54}Co were investigated with the ^{54}Fe$(p,n\gamma)^{54}$Co fusion evaporation reaction at the FN-TANDEM accelerator in Cologne. $\gamma\gamma$-coincidences, $\gamma\gamma$-angular correlations, and Compton asymmetries were measured. 28 low spin states were observed. 19 for the first time, eight new spin assignments and six new parity assignments were made, and seven γ-branching ratios were measured for the first time. $M1$ and $E2$ transition strengths between low-lying states in ^{54}Co were calculated in the shell-model framework. The experimental branching ratios and multipole mixing ratios indicate the existence of very strong isovector $M1$ transitions.

PACS number(s): 21.10.Hw, 23.20.Lv, 23.20.Gq, 27.40.+z

I. INTRODUCTION

Self-conjugate nuclei, which have equal numbers of neutrons and protons ($N=Z$), are particularly interesting objects. $N=Z$ nuclei are the most symmetric systems with respect to the isospin degree of freedom and thus allow us to test sensitively the isospin symmetry of the nuclear forces. Only in $N=Z$ nuclei can one study nuclear states with the lowest possible isospin quantum number $T=0$. Particularly interesting are odd-odd $N=Z$ nuclei with mass numbers $A \approx 40$–60. In these nuclei one finds that the lowest $T=1=T_{min}+1$ states are below the $T=0=T_{min}$ states or nearly degenerate as in ^{58}Cu. This is one of the many interesting properties of odd-odd self conjugate nuclei. The structure of $N=Z$ nuclei is sensitive to certain parts of the nuclear forces as shown, e.g., by the Wigner energy [1]. Therefore the structure of $N=Z$ nuclei is at present a very actively [2–11] studied topic in nuclear structure physics. For comparison to model calculations it is important to identify the low lying $T=0$ and $T=1$ states and to measure their properties.

In this work we have investigated the low-spin structure of the odd-odd $N=Z$ nucleus ^{54}Co up to an excitation energy of 4 MeV. We have considerably enlarged the hitherto known low spin level scheme of ^{54}Co [12–18]. We have performed shell model calculations using a residual surface delta interaction (SDI). Good agreement with experiment is obtained for branching ratios and multipole mixing ratios of the yrast states.

II. EXPERIMENTAL DETAILS AND RESULTS

Excited states of ^{54}Co were populated in the ^{54}Fe$(p,n\gamma)^{54}$Co fusion evaporation reaction. The proton beam was provided by the Cologne FN-TANDEM accelerator. Five Compton-suppressed Ge detectors and one Compton-suppressed CLUSTER detector were used in the COLOGNE-COINCIDENCE-CUBE-spectrometer. Two of the Ge detectors were mounted in forward direction at an angle $\theta=45°$ with respect to the beam axis. Another two were mounted in the backward direction at an angle $\theta=135°$ with respect to the beam axis. The fifth Ge detector and the CLUSTER detector were placed at an angle $\theta=90°$ below and above the beam line, respectively. Single γ spectra and $\gamma\gamma$-coincidence spectra of the depopulating γ cascades in ^{54}Co were measured with high energy resolution. As an example of the data, Fig. 1 shows the γ spectrum observed in coincidence with the decay of the $J^\pi=1^+$, $T=0$ state to the ground $J^\pi=0^+$, $T=1$ state in ^{54}Co. From the $\gamma\gamma$-coincidence relations a low spin level scheme of ^{54}Co was constructed, which is displayed in Fig. 2. We observed 28 levels and 42 γ transitions in this nucleus. With respect to earlier spectroscopic work [12–18] 29 γ transitions and 19 levels are new. In order to assign spin and parity quantum numbers we analyzed the $\gamma\gamma$-angular correlation information and the polarization information obtained with the composite CLUSTER detector. The angular correlation pattern is determined by the spin quantum numbers of the levels involved in a cascade, by the Gaussian width σ of the m-substate distribution of the initial level and by the multipole character of the corresponding γ radiation. The analysis of the $\gamma\gamma$-angular correlations resulted in six new unambiguous spin assignments, namely for the levels at 1614 keV ($J^\pi=1^+$), 1822 keV ($J^\pi=3^+$), 2174 keV ($J^\pi=3^+$), 2290 keV ($J=3$), 2852 keV ($J^\pi=4^+$), and 2919 keV ($J=3$). If we use the spin and parity assignment $J^\pi=7^+$ of the isomer at 197 keV, given in Ref. [18], we can, moreover, give unambiguous spin assignments for the levels at 1887 keV ($J^\pi=5^+$) and 2652 keV ($J^\pi=4^+$). The spin quantum numbers 1 and 2 for the levels at 937 keV and 1446 keV given in Ref. [18] could be confirmed in our analysis. As an example we show in Fig. 3 the experimental values of the $\gamma\gamma$-angular correlation of the 559.6–1614.1 keV cascade together with the fitted values for two different spin hypotheses. The number of different correlation groups results from the geometry of the COLOGNE-OSIRIS-COINCIDENCE-cube-spectrometer [19]. The 559.6–1614.1 keV cascade connects the level at 2174 keV, which could be assigned $J^\pi=3^+$ via the angular correlation of the 727.8–508.8 keV cascade, with the $J^\pi=0^+$ ground state. It is evident from the figure, that with a spin value of 2 for the intermediate level at 1614 keV the experimental values cannot be reproduced by the fit ($\chi^2_{min}=15.8$) for any possible value of the multipole mixing ratio δ of the $3^+ \rightarrow 2^+$ transition. In contrast to this with a spin value of J

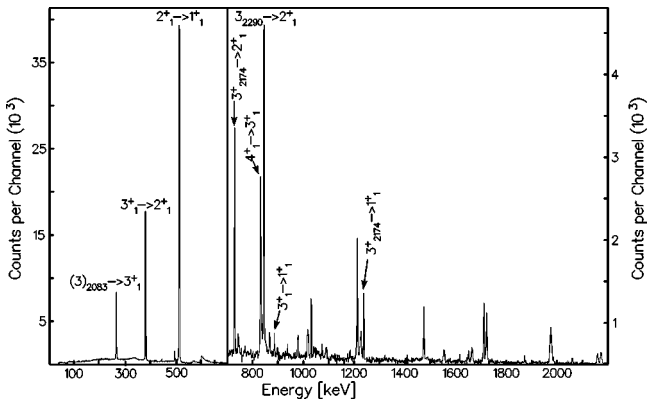

FIG. 1. $\gamma\gamma$ coincidence spectrum observed in the ^{54}Fe(p,n) fusion evaporation reaction. This coincidence spectrum is obtained by requiring a coincidence condition with the 937 keV $1^+_1 \rightarrow 0^+_1$ transition in ^{54}Co. For the left and the right part of the spectrum a different scale for the counts was used to improve the visibility of the high energy γ lines.

$=1$ for the level at 1614 keV, the fitted values are in good accordance with the experimental ones ($\chi^2_{min}=0.8$). Besides the spin quantum numbers of the excited states, the measured $\gamma\gamma$ angular correlations also give information on the multipole mixing ratios of the involved γ transitions (see Table I).

For six out of the eight levels, to which we assigned a spin value, we could also deduce the parity. In five cases (the levels at 1614, 1822, 1887, 2174, and 2652 keV) this assignment was based on the electric or magnetic character of the depopulating γ transitions. To determine this character, the CLUSTER detector was used as a Compton polarimeter. The sum of two coincident detector signals, which stem from the Compton scattering of an initial γ quantum in one segment of the CLUSTER and the subsequent absorption in another segment, carries the full energy information of the initial γ ray. The geometry of the Compton scattering process depends on the polarization of the initial γ ray with respect to the beam. Therefore observable asymmetries of the Compton scattering process allow us to measure the γ polarizations and the radiation character. Although its seven large volume Ge crystals are not arranged in the usual orthogonal way, numerical simulations [20] as well as experimental tests [21] have shown that the figure of merit for the CLUSTERS capability to measure polarizations can be even somewhat larger at high γ-ray energies than that of orthogonal five-crystal arrangements [22] or segmented crystals [23], compensating the loss of polarization sensitivity by its large absolute efficiency. Figure 4 shows the configuration of the CLUSTER with respect to the beam line in the present experiment. This configuration leads to three different scattering planes for the Compton scattering of γ rays between adjacent segments of the CLUSTER. In our experiment these scattering planes enclosed an angle of 15°, 75°, and 135° with the reaction plane, respectively. We analyzed coincidence-events between pairs of segments in the 15° and in the 75° scattering plane. The sum energy of the two coincident signals was sorted in two different spectra depending on to which scattering plane the involved pair of segments corresponds. If we denote the intensities in these two spectra by $I_{15°}$ and $I_{75°}$, respectively, the experimental asymmetry is defined as [21]

$$A_{exp}=\frac{I_{75°}-I_{15°}}{I_{75°}+I_{15°}}\approx Q^{Pol}P, \tag{1}$$

where Q^{Pol} denotes the positively defined polarization sensitivity of the CLUSTER and P is the linear polarization of the incoming photon with respect to the given geometry. Since the sign of the linear polarization sgn(P) determines the character of the electromagnetic radiation, with Eq. (1) we can conclude this character from the sign of the experimental asymmetry sgn(A). To illustrate the experimental asymmetries, Fig. 5 shows the difference spectrum of the 75° and the 15° spectrum. The parity assignment for the level at 2852 keV was based on the nonvanishing multipole mixing ratio of the 1029.6 keV transition to the 3^+ level at 1822 keV and the dominant magnetic character of this $\Delta J=1$ transition deduced from the measured multiple mixing ratio. A summary of the energy levels with certain spin and parity

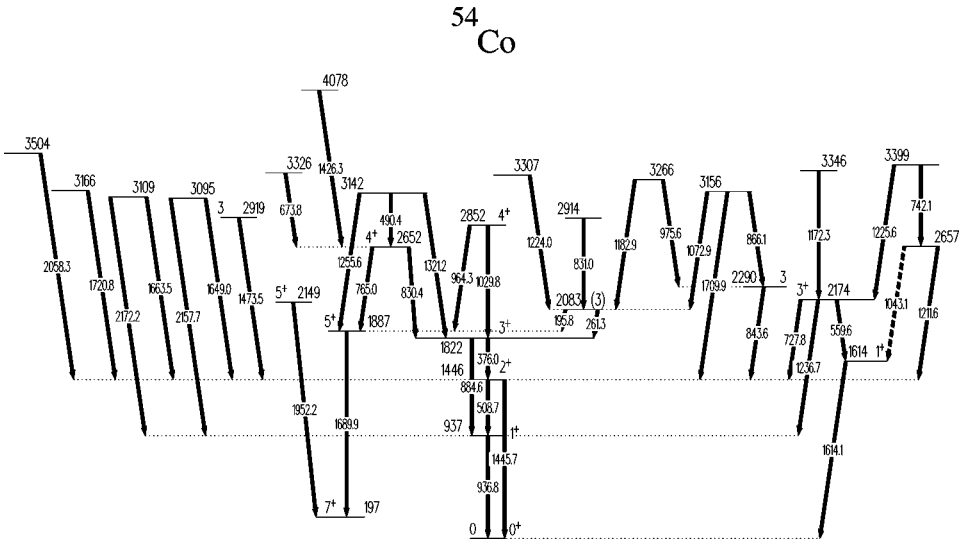

FIG. 2. Low spin level scheme of ^{54}Co from the $\gamma\gamma$ coincidence relations obtained in the ^{54}Fe$(p,n\gamma)^{54}$Co reaction at 13 MeV beam energy.

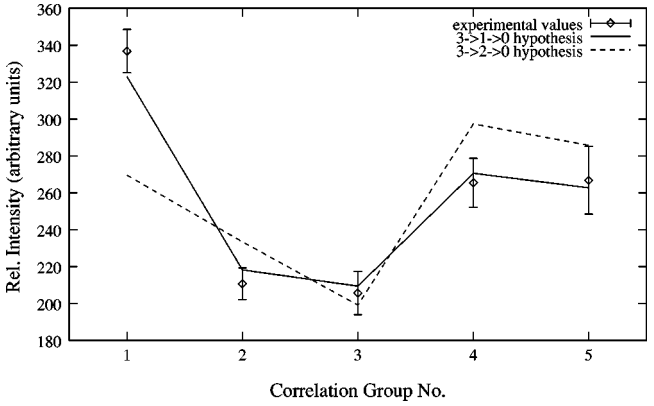

FIG. 3. Experimental and fitted values of the $\gamma\gamma$-angular correlation of the 559.6–1614.1 keV cascade which connects the 3^+ level at 2174 keV with the 0^+ ground state. Only the $J=1$ spin hypothesis for the intermediate level at 1614 keV can account for the observed correlation pattern. The fitted multipole mixing ratio for the $3^+ \rightarrow 1^+$ transition is $\delta=0.03(6)$, which supports pure $E2$ radiation and the same parities for the 3^+ and the 1^+ state.

values and with their depopulating γ transitions and branching ratios is given in Table I. Figure 6 shows an excerpt of the full level scheme including only those low-spin states with unique spin or parity quantum numbers. The assignment of the isospin quantum number $T=1$ is done by comparing the energies of the $T=1$ states with the energies of the corresponding states of the $T=1$ isospin multiplet in the nuclei ^{54}Ni and ^{54}Fe. The states of ^{54}Co, which have isospin $T=1$ and spin and parity quantum numbers $J^\pi=0^+$, 2^+, 4^+, form isospin triplets with the positive parity $T=1$ even spin states of the neighboring isobars ^{54}Ni and ^{54}Fe. From isospin symmetry we expect therefore that the excitation energies of the corresponding states are close in all three nuclei. The two lowest excited states in ^{54}Fe are the $J^\pi=2_1^+$ state at 1408 keV and the $J^\pi=4_1^+$ state at 2538 keV. From the absolute excitation energies of the 2_1^+ states in ^{54}Fe (1408 keV) and in ^{54}Co (1446 keV) one can assign the isospin quantum number $T=1$ to the 2_1^+ state in ^{54}Co. No other state with firm spin and parity assignment 2^+ is known in ^{54}Co. The $J^\pi=4^+$ excited state at 2652 keV in

TABLE I. We give the excitation energy E_i, spin, parity, and isospin quantum numbers I_i^π, T_i of the initial levels, the measured γ-transition energies E_γ and the excitation energy E_f and the quantum numbers for the final levels. The last three columns denote the radiation character Π (E=electric, M=magnetic), the relative intensity ratio I_γ and the $E2/M1$ multipole mixing ratio δ.

E_i (keV)	I_i^π, T_i $\hbar$	E_γ (keV)	E_f (keV)	I_f^π, T_f $\hbar$	Π	I_γ %	δ
937	$1_1^+,0$	936.8(2)	0	$0_1^+,1$	M		
1446	$2_1^+,1$	508.7(2)	937	$1_1^+,0$	M	100(2)	0.02(3)
		1445.7(2)	0	$0_1^+,1$	E	10.4(3)	
1614	$1_2^+,0$	1614.1(2)	0	$0_1^+,1$	M		
1822	$3_1^+,0$	376.0(2)	1446	$2_1^+,1$	M	100(3)	-0.01(5)
		884.6(4)	937	$1_1^+,0$	E	2.2(3)	
1887	$5_1^+,0$	1689.9(2)	197	$7_1^+,0$	E		
2083	(3)	261.3(2)	1822	$3_1^+,0$		100(3)	
		195.8(2)	1887	$5_1^+,0$		42(4)	
2149	$5_2^+,0$	1952.2(3)	197	$7_1^+,0$			
2174	$3^+,0$	728.0(3)	1446	$2_1^+,1$	M	100(10)	0.01(5)
		559.6(2)	1614	$1_2^+,0$	E	97(10)	
		1236.7(2)	937	$1_1^+,0$	E	55(9)	
2290	(3),0	843.6(2)	1446	$2_1^+,1$			-0.03(4)
2652	$4_1^+,(1)$	830.4(2)	1822	$3_1^+,0$	M	100(3)	-0.02(3)
		765.0(2)	1887	$5_1^+,0$	M	57(2)	0.04(6)
		1206.4(3)	1446	$2_1^+,1$	E	<2	
2852	$4_2^+,(0)$	1029.8(2)	1822	$3_1^+,0$	M/E	100(3)	0.10(4)
		964.3(2)	1887	$5_1^+,0$		51(3)	

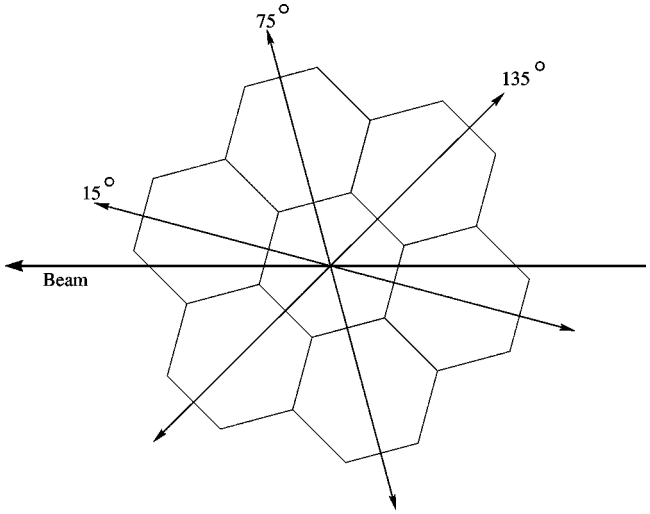

FIG. 4. Configuration of the CLUSTER detector in the present experiment.

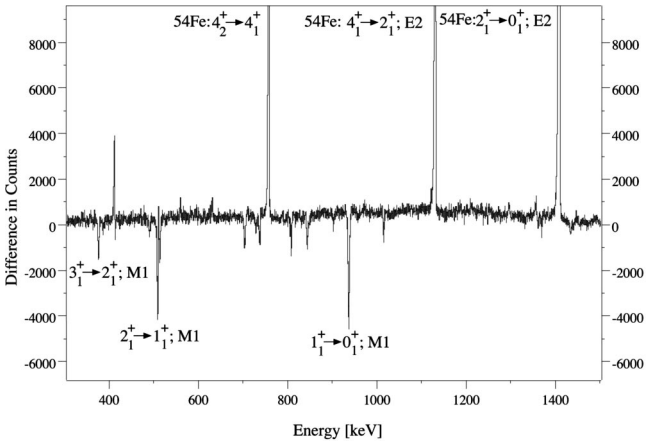

FIG. 5. Difference spectrum $I_{75^\circ}-I_{15^\circ}$ for initial γ rays, which were Compton scattered and then fully absorbed in two different crystals of the composite CLUSTER detector with a relative arrangement of 75° or 15° with respect to the beam axis (see text). One expects a positive difference $I_{75^\circ}-I_{15^\circ}$ for dominantly electric radiation (e.g., $E2$) and a negative difference for dominant magnatic radiation (e.g., $M1$). The largest differences are labeled with the corresponding transitions.

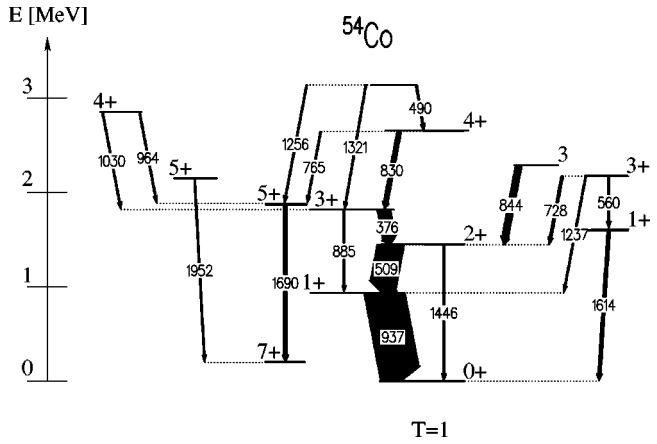

FIG. 6. Part of the level scheme, including those levels for which definite spin or parity quantum numbers are known. The width of the arrows corresponds to the relative intensity of the γ transitions. All levels not labeled $T=1$ are $T=0$ levels.

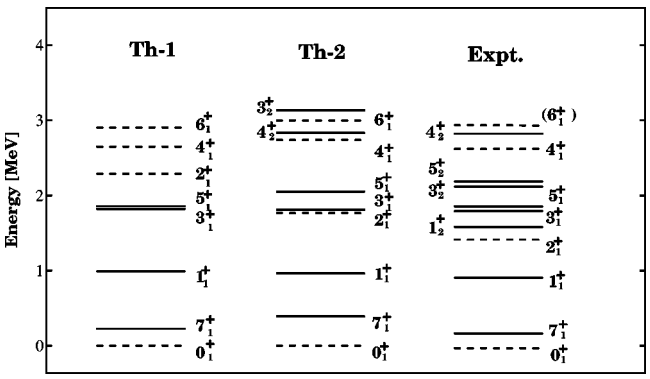

FIG. 7. Comparison of calculated and experimental spectra of the $J^\pi=0^+-7^+$ states in ^{54}Co. Th-1 and Th-2 label the calculations within $(f_{7/2})$ and $(f_{7/2},p_{3/2})$ configurational spaces, respectively. The states with isospin quantum number $T=1$ are plotted with dashed lines and $T=0$ with solid lines.

^{54}Co can be tentatively identified as $T=1$, $J^\pi=4_1^+$ state. This identification is based on the excitation energy ratios $E_x(4^+)/E_x(2^+)$ in ^{54}Co $[E_x(4^+)/E_x(2^+)=1.834]$ and in ^{54}Fe $[E_x(4^+)/E_x(2^+)=1.803]$ and on the pure $M1$ transition to the lower lying 3^+ and 5^+ states. However, we cannot rule out that the nearby $J^\pi=4^+$ state at 2852 keV is the $T=1$ state.

III. DISCUSSION

It is worthwhile to compare the rich data on γ transitions, branching ratios, and multipole mixing ratios to shell model calculations. Spherical shell model calculations with the residual surface delta interaction (SDI) [24,25] have been carried out for ^{54}Co considering ^{56}Ni as the inert core. At first only the proton $\pi f_{7/2}$ and neutron $\nu f_{7/2}$ valence orbitals were taken into account. The $f_{7/2}$ orbital is well separated from the lower lying sd shell (5 MeV) and the next higher lying orbital is $p_{3/2}$ (4 MeV) [26]. The valence orbital $f_{7/2}$ is occupied with one proton hole and one neutron hole. Within this limited configurational space proton and neutron holes couple to the even-spin $(J=0,2,4,6)$ $T=1$ multiplet and odd-spin $(J=1,3,5,7)T=0$ multiplet. The residual nucleon-nucleon interaction that was used in the present calculations has the form

$$V_{SDI}(\mathbf{r}_1,\mathbf{r}_2)=-\sum_{T=0}^{T=1}\{4\pi A'_T\delta(\Omega_{12})\delta(r_1-R)\delta(r_2-R)+B[2T(T+1)-3]\}, \quad (2)$$

where Ω_{12} is the angle between the interacting particles, $R=1.2A^{1/3}$fm is the nuclear radius, $A'_{T=0}$ and $A'_{T=1}$ are the two strength constants of the SDI for the two possible isospin quantum numbers. The parameter B adjusts the shift of the $T=0$ and $T=1$ centroids of level energies. The SDI parameters $A'_{T=0}$ and $A'_{T=1}$ regulate the splitting of the odd-spin states and even spins, respectively. Using such a simple interaction as the SDI and $f_{7/2}$ model space we can only reproduce the excitation energies of the yrast states with $J<7$. The excitation energy of the 7_1^+ is not satisfactorily obtained. This problem remains also for the enlarged configurational space which besides the $f_{7/2}$ configuration also takes into account the one-nucleon excitations to the $p_{3/2}$ orbital. Therefore the $\langle J^\pi=7^+|V_{SDI}|J^\pi=7^+\rangle_{B=0}$ matrix element for the $f_{7/2}$ shell is replaced with $1.93\langle J^\pi=7^+|V_{SDI}|J^\pi=7^+\rangle_{B=0}$ in order to reproduce the experimentally observed 0.197 MeV excitation energy of the $J^\pi=7^+$ state (see Fig. 7).

The calculated excitation energies of the low-lying states which do not have $\pi f_{7/2}^{-1}\times\nu f_{7/2}^{-1}$ character are much higher and are not shown in Fig. 7 excepting the 3_2^+ and 4_2^+ states. As shown in Ref. [26], relatively good agreement with experimental data can be achieved for some $f_{7/2}$ nuclei using empirical two-body matrix elements (m.e.) instead of the SDI matrix elements. Using these empirical m.e. we can reproduce energies better but the wave functions do not differ very much from the SDI wave functions. Thus for the calculation of electromagnetic (e.m.) transitions between low-spin states we can use the simple SDI.

For the case of the single-j-shell configurational space the e.m. transition probabilities are interaction independent.

TABLE II. The interaction parameter of the surface delta interaction as defined in Ref. [25], the single particle energies of the orbits included and effective e_p and e_n charges.

Theory	Parameter values (MeV)									e_p	e_n
	$A_{T=1}^{pp}$	$A_{T=1}^{nn}$	$A_{T=1}^{pn}$	$A_{T=0}^{pn}$	B	$\varepsilon_{\pi f_{7/2}}$	$\varepsilon_{\pi p_{3/2}}$	$\varepsilon_{\nu f_{7/2}}$	$\varepsilon_{\nu p_{3/2}}$		
Th-1	0.75	0.75	0.75	0.75	0.11	0.0		0.0		2.79	2.00
Th-2	0.75	0.75	0.65	0.65	0.11	0.0	3.9	0.0	3.9	1.77	1.11

TABLE III. Calculated electromagnetic transition strengths, experimental and calculated branching ratios and multipole mixing ratios δ in ^{54}Co. The experimental energies were used for calculations of branching ratios. The results are shown for the effective spin g factors $g_s^{\rm eff}=0.7\cdot g_s^{\rm free}$. The effective proton and neutron charges are given in Table II. In the fourth column the measured $R_{exp}(J_i)$ values defined by Eq. (3) are given (see text).

$(J_i,T_i)\rightarrow(J_f,T_f)$	$B(E2;J_i\rightarrow J_f)$, $[e^2\mathrm{fm}^4]$		$B(M1;\ J_i\rightarrow J_f)$, $[\mu_N^2]$		$R_{exp}(J_i)$	Branching ratio			δ		
	Th-1	Th-2	Th-1	Th-2		Expt.	Th-1	Th-2	Expt.	Th-1	Th-2
$(1_1^+,0)\rightarrow(0_1^+,1)$	0	0	4.05	3.81			100	100			
$(2_1^+,1)\rightarrow(1_1^+,0)$	1.0	0.4	4.63	4.17	4.2(1)	100(2)	100	100	0.02(3)	0.002	0.001
$(2_1^+,1)\rightarrow(0_1^+,1)$	126	129	0	0		10.4(3)	9.1	10.3			
$(3_1^+,0)\rightarrow(2_1^+,1)$	2.6	1.1	4.55	4.22	4.1(5)	100(3)	100	100	-0.01(5)	0.002	0.002
$(3_1^+,0)\rightarrow(1_1^+,0)$	141	129	0	0		2.2(3)	2.2	2.0			
$(3_2^+,0)\rightarrow(2_1^+,1)$		0.014		0.028		100(10)		100	0.01(5)		0.004
$(3_2^+,0)\rightarrow(1_1^+,0)$		3.5		0		55(9)		7			
$(3_2^+,0)\rightarrow(1_2^+,0)$		13		0		97(10)		1			
$(4_1^+,1)\rightarrow(3_1^+,0)$	4.3	2.2	4.12	3.58	>1.9	100(3)	100	100	-0.02(3)	0.007	0.005
$(4_1^+,1)\rightarrow(2_1^+,1)$	125	94	0	0		<2	0.9	0.8			
$(4_1^+,1)\rightarrow(5_1^+,0)$	7.3	2.6	4.28	3.81	>1.1	57(2)	82	78	0.04(6)	0.008	0.005
$(4_2^+,0)\rightarrow(3_1^+,0)$		1.4		0.004		100(3)		100	0.10(4)		0.11
$(4_2^+,0)\rightarrow(5_1^+,0)$		86.5		0.007		51(3)		252			

Thus the $M1$ and $E2$ transitions are more convenient tools for testing the nuclear structure than the energies. Therefore we focus our attention only on the $M1$ and $E2$ transition probabilities between low-lying states. From the data we know some branching ratios and multipole mixing ratios δ, which are given in Table I. Our first aim is to compare these observables with the shell model predictions.

In order to calculate e.m. transitions in the shell model we have to know the effective g factors for the $M1$ transition operator and effective charges for the quadrupole transition operator. We have done two calculations labeled Th-1 and Th-2. The configurational space of Th-1 contains only the $f_{7/2}$ shell. The Th-2 contains an enlarged configurational space that includes the $2p_{3/2}$ orbital with the restriction that it can be occupied with one proton and one neutron.

The quenching factor $\alpha_q=0.7$ for the effective proton and neutron spin g factors ($g_s^{\rm eff}=\alpha_q g_s^{\rm free}$) was taken from Ref. [26] while the orbital g factors remain free ($g_p^l=1.0,\quad g_n^l=0.0$) for both calculations. The effective proton e_p and neutron e_n charges were chosen to get the best agreement with experimental branching ratios for both calculations. The effective charges, single particle energies, and interaction parameters[1] for the Th-1 and Th-2 calculations are given in Table II.

Using these parameters we have calculated $B(M1)$ and $B(E2)$ values between the low-lying states, and with these $B(M1)$ and $B(E2)$ values we have obtained the branching ratios. The calculated branching ratios are compared with our corresponding experimental values in Table III.

We obtain good agreement for the branching ratios for the transitions between the states with the rather pure $\pi(f_{7/2}^{-1})\times\nu(f_{7/2}^{-1})$ configuration. We obtain also agreement within the experimental errors for the mixing ratios δ for the transitions between the $\pi(f_{7/2}^{-1})\times\nu(f_{7/2}^{-1})$ states.

If we suppose that the experimentally observed 3^+ state at 2174 keV and the 4^+ state at 2852 keV are the shell model $3_2^+,T=0$ state and the $4_2^+,T=0$ state, respectively, with the main $(\pi f_{7/2}^{-2}\times\nu f_{7/2}^{-1})\times\pi(p_{3/2}^1)$ and $(\pi f_{7/2}^{-1}\times\nu f_{7/2}^{-2})\times\nu(p_{3/2}^1)$ components, we obtain agreement with the experimental values as shown in Table III. The $E2/M1$ multipole mixing ratios δ for the transitions from the 4_2^+ state to the 3_1^+ state and from the 3_2^+ state to the 2_1^+ state are in good agreement with experiment. However, the $3_2^+\rightarrow1_2^+$ and $3_2^+\rightarrow1_1^+$ transitions are calculated to be much weaker and the $4_2^+\rightarrow5_1^+$ transition is calculated to be much stronger than the corresponding observed transitions. This means that other configurations that include $2p_{3/2}$, $2p_{1/2}$, and $1f_{5/2}$ orbitals are important for the 1_2^+, 3_2^+, and 4_2^+ states.

Based on the rather good agreement for the yrast states, we can now use the shell model to make some general predictions for $M1$ and $E2$ transitions between the states with the main $(\pi f_{7/2}^{-1}\times\nu f_{7/2}^{-1})_{J,T}$ configurations. These predictions are given in Table III. We note that the $(\pi f_{7/2}^{-1}\times\nu f_{7/2}^{-1})_{J,T}$ states fall in two classes with isospin $T=0$ and $T=1$: $T=1$, $J^\pi=0^+$, 2^+, 4^+, 6^+, and $T=0$, $J^\pi=1^+$, 3^+, 5^+, and 7^+. From our calculations given in Table III we note the following predictions:

(i) The isoscalar $\Delta T=0,\quad \Delta J=2$ transitions have large $B(E2)$ values. We note further that $B(E2)$ values for the $2_1^+\rightarrow0_1^+$ and $3_1^+\rightarrow1_1^+$ transitions are rather similar.

(ii) The isovector $\Delta T=1,\quad \Delta J=1$ transitions between $(\pi f_{7/2}^{-1}\times\nu f_{7/2}^{-1})_{J,T}$ states have large $B(M1)$ values and small

[1]The fitted interaction parameters $A_T^{\rho,\rho'}$ are connected to those from Eq. (1) by the following expression: $A_T^{\rho,\rho'}=A_T'\langle\delta(r_\rho-R)\delta(r_{\rho'}-R)\rangle$, where the radial matrix element $\langle\delta(r_\rho-R)\delta(r_{\rho'}-R)\rangle$ is supposed to be independent of the single particle states involved (see, for details, Ref. [25]).

$B(E2)$ values. The shell model predicts $B(M1;\ 0^+\rightarrow 1^+)=12.15\ \mu_N^2$ for ^{54}Co. We compare this value with the $\Delta T=1, 0^+\rightarrow 1^+$ $M1$ transition in ^{6}Li for which the reduced transition strength $B(M1;\ 0^+,\ T=1\rightarrow 1^+,\ T=0)=15.4(3)\ \mu_N^2$ is known experimentally [27]. These $M1$ transitions belong to the strongest known magnetic dipole transitions between bound nuclear states. They are caused by the constructive interference of the spin and orbital parts of the $M1$ matrix elements between the *quasideuteron* configurations formed by one proton and one neutron in the $j=l+1/2$ subshell [28].

It is tempting to try to extract also the large $B(M1;\ 2_1^+,\ T=1\rightarrow 1_1^+,\ T=0)$ and $B(M1;\ 3_1^+,\ T=0\rightarrow 2_1^+,\ T=1)$ values more directly from our data on the branching ratios from the gamma decay of the 2_1^+ and the 3_1^+ states given in Table I. In order to do this we need to know the absolute $B(E2;\ 2_1^+,\ T=1\rightarrow 0_1^+,\ T=1)$ and $B(E2;\ 3_1^+,\ T=0\rightarrow 1_1^+,\ T=0)$ values. These values are not known. We know, however, the $B(E2;\ 2_1^+,\ T=1\rightarrow 0_1^+,\ T=1)$ in the $T=1$ isospin partner nucleus ^{54}Fe. It amounts to $129(5)e^2\mathrm{fm}^4$ [29]. Assuming that $\Delta T=0$ $E2$ transition strengths between isobaric analogue states are close, we will judge the strengths of isovector $M1$ transitions in ^{54}Co from the measured branching ratios and the measured $B(E2)$ strength in ^{54}Fe. For this purpose it is convenient to define the following experimental quantity:

$$R_{exp}(J)=129\frac{B(M1;J\rightarrow J-1)/\mu_N^2}{B(E2;J\rightarrow J-2)/e^2\mathrm{fm}^4}=f(E_{\gamma 1},E_{\gamma 2},\delta_1,\delta_2)\frac{I_{\gamma 1}(J\rightarrow J-1)}{I_{\gamma 2}(J\rightarrow J-2)},\qquad(3)$$

which is proportional to the measured intensity branching ratio to the final states with $J_f=J_i-1$ and J_i-2. The proportionality factor $f(E_{\gamma 1},E_{\gamma 2},\delta_1,\delta_2)$ involves the observed γ energies and the $E2/M1$ multipole mixing ratios. The measured $R_{exp}(J)$ values are shown in Table III. Let us now judge absolute $B(M1)$ values in ^{54}Co from the measured quantities $R_{exp}(J)$ and the assumption $B(E2;\ ^{54}\mathrm{Co},\Delta T=0,\ J\rightarrow J-2)\approx B(E2;\ ^{54}\mathrm{Fe},\ 2_1^+\rightarrow 0_1^+)$ for $J=2$ and 3. *Under this assumption* the $R_{exp}(J)$ values equal the $B(M1;\ \ J\rightarrow J-1)$ values in units of μ_N^2. The $R_{exp}(J)$ values compare rather well with the corresponding shell model $B(M1)$ values (see columns 3 and 4 in Table III). This supports the dominant $(\pi f_{7/2}^{-1}\times\nu f_{7/2}^{-1})_{J,T}$ structure of the 1^+, 2^+, 3^+, and 4^+ yrast states in ^{54}Co. But while comparing the measured $R_{exp}(J)$ to the calculated $B(M1)$ values we must keep in mind that this identification relies on the postulated equality of the $B(E2;\ 2_1^+\rightarrow 0_1^+)$ values in ^{54}Co and ^{54}Fe, which is suggested from isospin symmetry.

IV. CONCLUSION

Summing up, we have investigated the low spin states in the odd-odd $N=Z$ nucleus ^{54}Co with the $^{54}\mathrm{Fe}(p,n\gamma)^{54}\mathrm{Co}$ fusion evaporation reaction. In the present experiment 19 low spin excitations were observed for the first time and eight new spin and six new parity assignments, were made. We have performed shell model calculations for the low-lying states in ^{54}Co using the SDI residual interaction and we have compared the results with the corresponding experimental quantities. The calculated branching ratios indicate that the 0_1^+, 1_1^+, 2_1^+, 3_1^+, and 4_1^+ excitations are predominant $\pi(f_{7/2}^{-1})\times\nu(f_{7/2}^{-1})$ seniority $\nu=2$ states. The 0_1^+, 2_1^+, and 4_1^+ states are the members of $T=1$ even spin multiplet and the 1_1^+ and 3_1^+ states are the members of the $T=0$ odd spin multiplet. The shell model yields large $\Delta T=0$ $E2$ transition strengths and large $\Delta T=1$ $M1$ transition strengths. From the calculated transition strengths we determined branching ratios for the yrast states, which agree very well with the data in most cases. Large scale shell model calculations in the complete fp-shell model space are needed to establish the above made assignments and to identify the structure of other nonyrast states.

ACKNOWLEDGMENTS

The authors want to thank in particular Mr. A. Fitzler, Mr. S. Kasemann, and Mr. H. Tiesler for help in data taking. We also thank Dr. A. Dewald, Dr. J. Eberth, Professor A. Gelberg, Professor T. Otsuka, Dr. D. Rudolph, and Dr. K.O. Zell for helpful discussions.

[1] P. Van Isacker and D. D. Warner, Phys. Rev. Lett. **78**, 3266 (1997).

[2] W. Satula and R. Wyss, Phys. Lett. B **393**, 1 (1997).

[3] C. E. Svensson, S. M. Lenzi, D. R. Napoli, A. Poves, C. A. Ur, D. Bazzacco, F. Brandolini, J. A. Cameron, G. de Angelis, A. Gadea, D. S. Haslip, S. Lunardi, E. E. Maqueda, G. Martínez-Pinedo, M. A. Nagarajan, C. Rossi-Alvarez, A. Vitturi, and J. C. Waddington, Phys. Rev. C **58**, R2621 (1998).

[4] D. Bucurescu, C. Rossi Alvarez, C. A. Ur, N. Marginean, P. Spolaore, D. Bazzacco, S. Lunardi, D. R. Napoli, M. Ionescu-Bujor, A. Iordachescu, C. M. Petrache, G. de Angelis, A. Gadea, D. Foltescu, F. Brandolini, G. Falconi, E. Farnea, S. M. Lenzi, N. H. Medina, Z. Podolyak, M. De Poli, M. N. Rao, and R. Venturelli, Phys. Rev. C **56**, 2497 (1997).

[5] S. Skoda, B. Fiedler, F. Becker, J. Eberth, S. Freund, T. Steinhardt, O. Stuch, O. Thelen, H. G. Thomas, L. Käubler, J. Reif, H. Schnare, R. Schwengner, T. Servene, G. Winter, V. Fischer, A. Jungclaus, D. Kast, K. P. Lieb, C. Teich, C. Ender, T. Härtlein, F. Kock, D. Schwalm, and P. Baumann, Phys. Rev. C **58**, R5 (1998).

[6] G. de Angelis, C. Fahlander, A. Gadea, E. Farnea, W. Gelletly, A. Aprahamian, A. Axelsson, D. Bazzacco, F. Becker, P. G. Bizzeti, A. Bizzeti-Sona, F. Brandolini, D. de Acuña, M. De Poli, J. Eberth, D. Foltescu, S. Lenzi, S. Lunardi, T. Martinez, D. R. Napoli, P. Pavan, C. M. Petrache, C. Rossi-Alvarez, D. Rudolph, B. Rubio, S. Skoda, P. Spolaore, G. Thomas, C. Ur, M. Weiszflog, and R. Wyss, Nucl. Phys. **A630**, 426 (1998).

[7] T. Otsuka, Michio Honma, and Takahiro Mizusaki, Phys. Rev. Lett. **81**, 1588 (1998).
[8] D. Rudolph, C. J. Gross, J. A. Sheikh, D. D. Warner, I. G. Bearden, R. A. Cunningham, D. Foltescu, W. Gelletly, F. Hannachi, A. Harder, T. D. Johnson, A. Jungclaus, M. K. Kabadiyski, D. Kast, K. P. Lieb, H. A. Roth, T. Shizuma, J. Simpson, O. Skeppstedt, B. J. Varley, and M. Weiszflog, Phys. Rev. Lett. **76**, 376 (1996).
[9] J. Terasaki, R. Wyss, and P. H. Heenen, Phys. Lett. B **437**, 1 (1998).
[10] S. M. Vincent, P. H. Regan, D. D. Warner, R. A. Bark, D. Blumenthal, M. P. Carpenter, C. N. Davids, W. Gelletly, R. V. F. Janssens, C. D. O'Leary, C. J. Lister, J. Simpson, D. Seweryniak, T. Saitoh, J. Schwartz, S. Törmänen, O. Juillet, F. Nowacki, and P. Van Isacker, Phys. Lett. B **437**, 264 (1996).
[11] C. Friessner, N. Pietralla, A. Schmidt, I. Schneider, Y. Utsuno, T. Otsuka, and P. von Brentano, Phys. Rev. C **60**, 011304 (1999).
[12] D. Rudolph, C. Baktash, W. Satula, J. Dobaczewski, W. Nazarewicz, M. J. Brinkman, M. Delvin, H.-Q. Jin, D. R. La Fosse, I. L. Riedinger, D. G. Sarantites, and C.-H. Yu, Nucl. Phys. **A630**, 417c (1998).
[13] B. D. Anderson, C. Lebo, A. R. Baldwin, T. Chittrakarn, R. Madey, J. W. Watson, and C. C. Foster, Phys. Rev. C **41**, 1474 (1990).
[14] K. M. Maeda, H. Orihara, T. Murakami, S. Nishihara, T. Nakagawa, K. Miura, and H. Ohnuma, Nucl. Phys. **A403**, 1 (1983).
[15] L. R. Medsker, L. V. Theisen, L. H. Fry, Jr., and J. S. Clements, Phys. Rev. C **19**, 790 (1979).
[16] R. R. Sankey, K. W. Kemper, H. S. Plendl, and J. W. Nelson, Phys. Rev. C **3**, 2273 (1971).
[17] N. S. P. King, C. E. Moss, H. W. Baer, and R. A. Ristinen, Nucl. Phys. **A177**, 625 (1971).
[18] Huo Junde, Nucl. Data Sheets **68**, 887 (1993).
[19] R. Wirowski, M. Schimmer, L. Esser, S. Albers, K. O. Zell, and P. von Brentano, Nucl. Phys. **A586**, 427 (1994).
[20] L. M. Garcia-Raffi, J. L. Tain, J. Bea, A. Gadea, L. Palafox, J. Rico, and B. Rubio, Nucl. Instrum. Methods Phys. Res. A **359**, 628 (1995).
[21] D. Weisshaar, diploma thesis, University of Cologne, 1996.
[22] B. Kasten, R. D. Heil, P. von Brentano, P. A. Butler, S. D. Hoblit, U. Kneissl, S. Lindenstruth, G. Müller, H. H. Pitz, K. W. Rose, W. Scharfe, M. Schumacher, U. Seemann, Th. Weber, C. Wesselborg, and A. Zilges, Phys. Rev. Lett. **63**, 609 (1989).
[23] B. Schlitt, U. Maier, H. Friedrichs, S. Albers, I. Bauske, P. von Brentano, R. D. Heil, R.-D. Herzberg, U. Kneissl, J. Margraf, H. H. Pitz, C. Wesselborg, and A. Zilges, Nucl. Instrum. Methods Phys. Res. A **337**, 416 (1994).
[24] A. Plastino, R. Arvieu, and S. A. Moszkowsk, Phys. Rev. **145**, 837 (1966).
[25] P. J. Brussard and P. W. M. Glaudemans, *Shell-Model Applications in Nuclear Spectroscopy* (North-Holland, Amsterdam, 1977).
[26] A. G. M. van Hees and P. W. M. Glaudemans, Z. Phys. A **303**, 267 (1981).
[27] P. M. Endt, At. Data Nucl. Data Tables **55**, 192 (1993).
[28] A. F. Lisetskiy, R. V. Jolos, N. Pietralla, and P. von Brentano, Phys. Rev. C **60**, 064310 (1999).
[29] W. Gongqing, Nucl. Data Sheets **50**, 255 (1987).